

Thin shell collapse in semiclassical gravity

Valentina Baccetti, Sebastian Murk, and Daniel R. Terno

Department of Physics & Astronomy, Macquarie University, Sydney NSW 2109, Australia

Contraction of a massive spherically-symmetric thin dust shell that separates a flat interior region from a curved exterior is the simplest model of gravitational collapse. Nevertheless, different extensions of this model that include a collapse-triggered radiation lead to contradictory predictions. Analysis of the boundary of a trapped spacetime region identifies two possible families of metrics — ingoing and outgoing Vaidya — that may describe geometry in its vicinity. Description of the exterior geometry using the outgoing Vaidya metric is known to result in horizon avoidance and timelike-to-null transition. We estimate the radial coordinate of this transition. Violation of the null energy condition (NEC) is the prerequisite for a finite-time formation of a trapped region according to a distant observer, and therefore only the outgoing Vaidya metric with decreasing mass is applicable in this case. Using this metric for the exterior geometry leads to a finite (proper or distant) time of horizon crossing. A macroscopic shell loses only a negligible amount of its rest mass in the process. However, this is incompatible with the NEC violation, thus rendering the horizon formation and its crossing by the shell impossible.

I. INTRODUCTION

Black holes were originally conceived as spacetime domains from where no signal can escape. Mathematically, these are defined as a complement of the causal past of the future null infinity [1–3], and their null boundaries are event horizons. General relativity (GR) and many modified theories of gravity predict black hole formation at the final stage of gravitational collapse. Event horizons are global teleological entities that are generically unobservable [4]. Instead, locally-defined surfaces provide a more suitable conceptual and calculational framework. A trapped region — a spacetime domain where both radial null geodesics have negative expansion — forms inside the collapsing matter. Its suitably defined boundary (apparent horizon or another related surface) asymptotically approaches the event horizon [1–5].

Classical matter that satisfies energy conditions [2, 6] crosses the event horizon and reaches the singularity in finite proper time τ (that we associate with an observer Alice that is co-moving with the collapsing matter). According to a distant outside observer (Bob) horizon formation takes an infinite amount of time. The trapped region and the associated surfaces are hidden behind the event horizon and thus cannot be observed by him. According to Bob the collapsing matter remains in a perpetual state of approach to the event horizon.

The simplest model of gravitational collapse is provided by contraction of a massive, infinitesimally thin dust shell. The thin shell formalism models narrow transitional regions between spacetime domains as hypersurfaces of discontinuity. Mathematical consistency is maintained by imposing joining rules, known as the junction conditions, for the solutions of the Einstein equations on both sides of the hypersurface [3]. For the collapse of a thin shell in an asymptotically flat spacetime the interior geometry is flat, and in classical GR the exterior geometry is described by the Schwarzschild metric. The simplicity of the model allows one to obtain the explicit time dependence of the shell’s radius $R(\tau)$, and to determine the point in time when the shell crosses the Schwarzschild radius, $R(\tau_c) = r_g = 2M$.

The emergence of variously defined horizons from regu-

lar initial data is already a formidable problem in classical GR [2, 5, 7]. Taking into account quantum effects, such as collapse-triggered radiation, complicates the analysis even further [8–11]. While it is known that radiation of this kind (sometimes referred to as “pre-Hawking radiation”) does not require formation of an event or even of an apparent horizon [12–14], its explicit form and the consequences are still controversial [14–17].

Thin shell are used to analyze various alternatives to black holes as the final stage of gravitational collapse [10, 18–20]. It allows one to circumvent some of the controversial issues, such as the structure of the energy-momentum tensor within the collapsing body. Moreover, the exterior metric naturally has a Schwarzschild radius that is initially located within the Minkowski interior. Thus one bypasses the problem of emergence of trapped surfaces and is able to model the radiation emission that precedes their formation.

Nevertheless, the results that were obtained so far appear contradictory. On the one hand, models that use the outgoing Vaidya metric, as well as general metrics that satisfy certain regularity conditions, exhibit horizon avoidance [21–25]. That is, for an arbitrary law that describes conversion of the shell’s mass to radiation, the gap $X := R - r_g$ always remains positive. However, the dynamics of these shells involves peculiarities [24, 25] that will be described below (Sec. III B). On the other hand, arguments that are based on the iterative evaluation of the effects of backreaction (starting with the results for the energy-momentum tensor of Hawking radiation on the background of an eternal black hole) showed that while the collapse duration is extended, the shell eventually crosses the event horizon in a finite time of both Alice and Bob [14].

The semiclassical analysis of the energy-momentum tensor near r_g for a general spherically symmetric collapse [26] demonstrated that, generically, the limiting forms of the tensor are only distinguished by two signs. The resulting near-horizon geometry is then described either by an outgoing or ingoing Vaidya metric with increasing or decreasing mass. Physically, the signs are determined by whether or not the null energy condition (NEC) [2, 6] is satisfied, and by the growth or shrinking of r_g . Using these results we resolve the apparent contradiction between the two sets of predictions for the final

state of the thin shell collapse. Furthermore, we derive quantitative limitations — well above the Planck scale — of both the thin shell models and the semiclassical formalism.

This paper is organized as follows. In the next Section we briefly recap the main features of the regularity analysis and metric classification near r_g . Section III first summarizes essential features of massive thin shell collapse in GR, and then presents the two cases of collapsing and evaporating shells. The consequences of our findings are discussed in Section IV.

To simplify the notation we label the quantities on the shell Σ by capital letters, e.g. $R := r|_{\Sigma}$, $F := f(U, R)$. The jump of a physical quantity A across the shell is written as $[A] := A|_{\Sigma_+} - A|_{\Sigma_-}$. All derivatives are explicitly indicated by subscripts, as in $A_R = \partial_R A(U, R)$. The total proper time derivative $dA/d\tau$ is denoted as \dot{A} , and the total derivative over some parameter λ is $A_\lambda := A_R R_\lambda + A_U U_\lambda$. The time t always refers to the coordinate time (proper time of Bob).

II. GENERAL PROPERTIES OF THE METRIC NEAR THE SCHWARZSCHILD SPHERE

We work within the framework of semiclassical gravity [14, 23]. That means we use the concepts of GR, and quantum effects are taken into account via the semiclassical Einstein equations,

$$R_{\mu\nu} - \frac{1}{2}Rg_{\mu\nu} = 8\pi\langle\hat{T}_{\mu\nu}\rangle, \quad (1)$$

where $R_{\mu\nu}$ is the Ricci tensor, and $\langle\hat{T}_{\mu\nu}\rangle \equiv T_{\mu\nu}$ is the expectation value of the stress-energy tensor. The latter represents the entire matter content of the model: both the collapsing matter and the created quantum field excitations are included. This cumulative representation allows a self-consistent study of the dynamics without having recourse to iterative calculations of the backreaction [9].

Three coordinate systems are particularly useful. We use the Schwarzschild radial coordinate r , and either the Schwarzschild time t , or the retarded and advanced null coordinates u and v , respectively. When the nature of the time coordinate is immaterial, we use the generic notation z . The most general spherically symmetric metric is given by

$$ds^2 = -e^{2h(t,r)}f(t,r)dt^2 + f(t,r)^{-1}dr^2 + r^2d\Omega \quad (2)$$

$$= -e^{2h^u(u,r)}f^u(u,r)du^2 - 2e^{h^u(u,r)}dudr + r^2d\Omega, \quad (3)$$

$$= -e^{2h^v(v,r)}f^v(v,r)dv^2 + 2e^{h^v(v,r)}dvdv + r^2d\Omega. \quad (4)$$

The function f is coordinate-independent [27], i.e., $f(t, r) = f^u(u(t, r), r)$, etc., and we can decompose it as

$$f = 1 - 2M(t, r)/r = 1 - 2M^u(u, r)/r. \quad (5)$$

In the following we drop the superscripts on f and M as it does not lead to confusion. The functions h , h^u and h^v play the role of integrating factors [27] that turn, e.g., the expression

$$dt = e^{-h}(e^{h^v}dv - f^{-1}dr), \quad (6)$$

into the exact differential, provided that the coordinate transformation exists [26].

In an asymptotically flat spacetime the time variable t is the proper time of a stationary Bob. In the following we work in this setting, but our results are also applicable to a cosmological background if there exists an intermediate scale $r_g \ll r \ll R$, where R is set by the cosmological model.

Two technical assumptions result in the classification of the energy-momentum tensor and the resulting metrics. First, we assume that trapped regions form at a finite time t of Bob. This entails that the equation $f(z, r) = 0$ has a solution. This solution, or, if there are several, the largest one, is the Schwarzschild horizon radius $r_g(z)$. Second, we require that the hypersurface $r = r_g$ is regular by demanding that the two curvature scalars that are directly obtained from the energy-momentum tensor,

$$T := T^\mu_\mu \equiv R/8\pi, \quad \mathfrak{T} := T^{\mu\nu}T_{\mu\nu} \quad (7)$$

are finite.

There are several possibilities for the stress-energy tensor behaviour close to the horizon to satisfy these requirements. The generic one (that is consistent with the known results of the energy-momentum tensor of Hawking radiation [8, 28]) results in the limiting form of the (tr) block of $T_{\mu\nu}$,

$$T_{\hat{a}\hat{b}} = \frac{\Xi}{f} \begin{pmatrix} 1 & s \\ s & 1 \end{pmatrix}, \quad (8)$$

where $s = \pm 1$ and we have used the orthonormal frame to simplify the expression. As a result, the geometry is described by a suitable Vaidya metric.

The Einstein equations only have real solutions if $\Xi = -\Upsilon^2 < 0$. Thus the energy-momentum tensor violates the NEC: $T_{\hat{a}\hat{b}}k^{\hat{a}}k^{\hat{b}} < 0$ for a radial null vector $k^{\hat{a}} = (1, s, 0, 0)$. The two possibilities — growth and contraction of the trapped region — are determined by the sign of T_t^r . These two cases are given in the first two rows of Table I. An evaporating black hole corresponds to the outgoing Vaidya metric with decreasing mass.

$\text{sgn}(T_{tt})$	$\text{sgn}(T_t^r)$	s	Vaidya metric
−	−	+	$(v, r) \quad M'(v) < 0$
−	+	−	$(u, r) \quad M'(u) > 0$
+	−	−	$(u, r) \quad M'(u) < 0$
+	+	+	$(v, r) \quad M'(v) > 0$

TABLE I. Signs in the limiting form of $T_{\mu\nu}$. The Einstein equations have real solutions only in the first two cases.

If the NEC is satisfied, then the Einstein equations cannot have real solutions and the Schwarzschild horizon r_g cannot be formed in finite time of a distant observer. Performing a formal transformation to (u, r) coordinates (in the case of evaporation, $T_t^r < 0$) and (v, r) coordinates when $T_t^r > 0$ leads to a very simple form of the Einstein equations whose solutions are the pure outgoing and ingoing Vaidya metric, respectively. This case is summarised in rows three and four of Table I [26].

III. THIN SHELL DYNAMICS

A. Classical thin shell formalism

We briefly review the collapse of a massive, spherically symmetric thin dust shell Σ in 3+1 dimensions [3, 23]. The metric across the two domains that it separates can be represented as the distributional tensor

$$\bar{g}_{\mu\nu} = \bar{g}_{\mu\nu}^+ \Theta(\xi) + \bar{g}_{\mu\nu}^- \Theta(-\xi), \quad (9)$$

using the set of special coordinates $\bar{x}^\mu = (w, \xi, \theta, \phi)$. Here $\Theta(\xi)$ is the step function and the interior and exterior metrics $\bar{g}^\pm(\bar{x})$ are continuously joined at $\xi = 0$. The coordinates w and ξ as well as the explicit form of this metric in a general spherically symmetric case are given in [25].

A mathematically equivalent approach is the thin shell formalism. It is particularly convenient for our purposes. Birkhoff's theorem imposes the Schwarzschild metric at the shell's exterior,

$$\begin{aligned} ds_+^2 &= -f(r_+) du_+^2 - 2du_+ dr_+ + r_+^2 d\Omega \\ &= -f(r_+) dv_+^2 + 2dv_+ dr_+ + r_+^2 d\Omega \\ &= -f(r_+) dt_+^2 - f^{-1}(r_+) dr_+^2 + r_+^2 d\Omega. \end{aligned} \quad (10)$$

where the subscript $+$ denotes the exterior region and the retarded and advanced null coordinates u and v are the Eddington-Finkelstein (EF) coordinates.

The interior region is described by the Minkowski metric,

$$\begin{aligned} ds_-^2 &= -du_-^2 - 2du_- dr_- + r_-^2 d\Omega \\ &= -dv_-^2 + 2dv_- dr_- + r_-^2 d\Omega \\ &= -dt_-^2 + dr_-^2 + r_-^2 d\Omega, \end{aligned} \quad (11)$$

where $u_- = t_- - r_-$, $v_- = t_- + r_-$. The shell's trajectory is parametrized by the proper time τ as $(T_\pm(\tau), R_\pm(\tau))$ or $(V_\pm(\tau), R_\pm(\tau))$ using, respectively, (t, r) or (v, r) coordinates outside and inside the shell. We use the hypersurface coordinates $y^\alpha = (\tau, \Theta := \theta|_\Sigma, \Phi := \phi|_\Sigma)$. The first junction condition [3], which is the statement that the induced metric h_{ab} is the same on the both sides of the shell Σ , $ds_\Sigma^2 = h_{ab} dy^a dy^b = -d\tau^2 + R^2 d\Omega_{D-1}$, leads to the identification $R_+ \equiv R_- =: R(\tau)$. Henceforth we drop the subscripts from the radial coordinate. Trajectories of the shell's particles are timelike, hence

$$\dot{U}_+ = \frac{-\dot{R} + \sqrt{F + \dot{R}^2}}{F}, \quad (12)$$

$$\dot{V}_+ = \frac{\dot{R} + \sqrt{F + \dot{R}^2}}{F}, \quad (13)$$

$$\dot{T}_+ = \frac{\sqrt{F + \dot{R}^2}}{F}, \quad (14)$$

where $F = 1 - r_g/R$. In the following we drop the subscript '+' from the exterior quantities.

The surface energy-momentum tensor of a massive thin dust shell is

$$S^{ab} = \sigma v^a v^b = \sigma \delta_\tau^\alpha \delta_\tau^b, \quad (15)$$

where σ is the surface density. The rest mass of the shell is $m = 4\pi\sigma R^2$. The second junction condition relates the jump in extrinsic curvature

$$K_{ab} := \hat{n}_{\mu;\nu} e_a^\mu e_b^\nu, \quad (16)$$

to the surface energy-momentum tensor,

$$S_{ab} = -([K_{ab}] - [K]h_{ab})/8\pi, \quad (17)$$

where $K := K_a^a$, and $[K] := K|_{\Sigma^+} - K|_{\Sigma^-}$ is the discontinuity of the extrinsic curvature scalar K across the two sides Σ^\pm of the surface.

The equation of motion for the shell can be obtained from

$$\begin{aligned} \mathcal{D}(R) := & \frac{2\ddot{R} + F'}{2\sqrt{F + \dot{R}^2}} - \frac{\ddot{R}}{\sqrt{1 + \dot{R}^2}} \\ & + \frac{\sqrt{F + \dot{R}^2} - \sqrt{1 + \dot{R}^2}}{R} = 0, \end{aligned} \quad (18)$$

while

$$-4\pi\sigma = \frac{\sqrt{F + \dot{R}^2} - \sqrt{1 + \dot{R}^2}}{R}, \quad (19)$$

directly describes the evolution of the surface density. For a collapse without change in the rest mass $m = \text{const}$ we have

$$r_g = 2m\sqrt{1 + \dot{R}^2} - m^2/R. \quad (20)$$

The trajectory is obtained by integration of

$$\dot{R} = -\sqrt{\left(\frac{r_g}{2m} + \frac{m}{2R}\right)^2 - 1}. \quad (21)$$

Using this result the equation of motion can be rewritten as

$$\ddot{R} = -\frac{1}{4R^2} \left(r_g + \frac{m^2}{R} \right). \quad (22)$$

B. Evaporating shell and positive energy density

The outgoing Vaidya metric with $M_u < 0$ is an excellent approximation to the geometry of an evaporating black hole for $r > 3r_g$ [8]. It is used to model the effects of backreaction in various settings [21–23, 29, 30]. However, the resulting energy-momentum tensor does not violate the NEC and cannot represent a setup where the trapped region has formed at a finite time of a distant observer. Presence of evaporation modifies the equation of motion,

$$\mathcal{D}(R) + \frac{F_U}{F\sqrt{F + \dot{R}^2}} \left(\frac{1}{2} - \dot{R}\dot{U} \right) = 0 \quad (23)$$

while Eq. (19) still holds [23, 25].

In the limit of large \dot{R} the asymptotic expression becomes

$$\ddot{R} \approx \frac{8M_U \dot{R}^4}{RF^2} \approx \frac{16MM_U \dot{R}^4}{X^2}, \quad (24)$$

where the second relation in Eq. (24) holds for $X \ll r_g$. In fact this accelerates the collapse, as can be seen in Fig. 3.

Despite this acceleration, the shell never crosses the ever-shrinking Schwarzschild sphere at $r = r_g$, as can be readily deduced by monitoring the gap

$$X := R - r_g. \quad (25)$$

Anticipating the transition to a null trajectory we use a generic parameter λ to describe the shell. It can be u_- [24] or R itself, as is common practice in the analysis of null shells [25]. Using Eq. (14), we find that close to r_g

$$U \approx -\frac{2R_\lambda}{F} \approx -\frac{2R_\lambda r_g}{X}, \quad (26)$$

where the first relation is exact for null shells and the second is valid for $x \ll r_g$.

Evaluating the derivative of X over λ we have

$$\begin{aligned} X_\lambda &= R_\lambda - \frac{dr_g}{dU} U_\lambda = -|R_\lambda| \left(1 - \left| \frac{dr_g}{dU} \right| \frac{2}{F} \right) \\ &\gtrsim -|R_\lambda| \left(1 + \frac{8|M_U|M}{X} \right). \end{aligned} \quad (27)$$

As a result the gap decreases only until $X \approx \epsilon_*$ [21–23], where

$$\epsilon_* := 2 \frac{dr_g}{dU} r_g = 8M|M_U|. \quad (28)$$

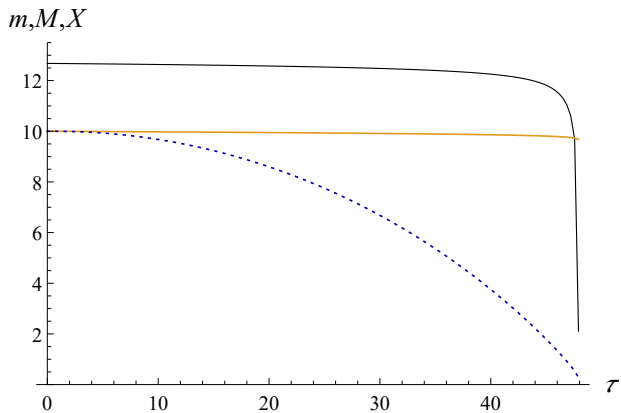


FIG. 1. Transition to the null trajectory. The orange line represents the gravitational mass $M(\tau) = r_g(\tau)/2$. The rest mass $m(\tau)$ is shown as the thin black line, and the gap $X(\tau) = R(\tau) - r_g(\tau)$ as the blue dotted line. For simulation purposes the evaporation was switched on at $\tau = u = 0$. The initial conditions are $R(0) = 30$ and $\dot{R}(0) = 0$, while $r_0 := r_g(0) = 20$, and $\alpha = 1$. The evaporation ends at the retarded time $u_* = r_0^3/3\alpha = 8000/3$, but the system breaks down at approximately $\tau_m = 47.912$, indicating transition to the null trajectory. At the transition most of the gravitational mass is still contained within the shell, $M(\tau_m)/M(0) = 0.968$, while the gap is $X(\tau_m) = 0.279$. The closest approach [25] is determined by $\epsilon_* = 0.1$, giving the estimate for the gap at the transition as $X_\infty = 0.25$.

However, horizon avoidance comes with a price. The shell sheds its rest mass and becomes null in finite proper time. It

was demonstrated in [24] for the outgoing Vaidya metric and in [25] for a general metric of Eq. (3) with $h(u, r) < +\infty$ and a general evaporation law. While the rest mass $m = 4\pi\sigma R^2$ becomes zero for a finite value of $R > r_g > 0$, for a macroscopic shell only a negligible fraction of the gravitational mass is lost up to the transition, i.e. $r_g \approx r_g(0) = \text{const}$. Fig. 1 illustrates this process for the Page-like evaporation law

$$\frac{dr_g}{du} = -\frac{\alpha}{r_g^2}. \quad (29)$$

Using the asymptotic form of the equation of motion as given by Eq. (24) we can estimate the transition radius. Since $r_g \approx r_0$, we have $\dot{X} \approx \dot{R}$, and thus

$$\ddot{X} = -\frac{2\epsilon_* \dot{X}^4}{X^2}. \quad (30)$$

The equation for $\tau(X)$ has a simpler form and can be solved by separation of variables if we approximate $\epsilon_* \approx \text{const}$. The first integration gives

$$\frac{d\tau}{dX} = -\frac{\sqrt{2(-2\epsilon_* + XK_1)}}{\sqrt{X}}, \quad (31)$$

where K_1 is the integration constant. Motion of the shell is affected by evaporation only at distances of the order of $X \ll r_g$. Within the range $r_g \gg X \gg \epsilon_*$, where the equation above is already applicable, we set the initial value of $d\tau/dX$ using the classical value of the radial velocity of the shell at the horizon crossing. From Eq. (21) we find $\dot{R} \sim -3/4$ for a shell initially at rest, giving $K_1 = 8/9$. At the timelike-to-null transition $d\tau/dX \rightarrow 0$, and therefore it occurs at

$$X_\infty \approx 2\epsilon_*/K_1 = 9\epsilon_*/4. \quad (32)$$

At this point the model must be supplemented by additional considerations since the unmodified dynamics would inevitably cause the shell to become tachyonic. There are three main scenarios that avoid the tachyonic solution: termination of the radiation (i.e. the metric outside the shell reverts to the Schwarzschild metric in EF coordinates) [24], modification of the metric such that the junction conditions for null shells are satisfied from the transition point onwards, or preservation of the Vaidya form of the metric and development of pressure that allows to maintain the null trajectory [25].

The first option restores the classical collapse that is completed in finite proper time of Alice and infinite proper time of Bob. In the second case the final fate of the shell depends on specific form of the new metric. The last option leads to horizon avoidance with or without appearance of a transient naked singularity.

C. Evaporating shell and negative energy density

Geometry near the apparent horizon of the contracting trapped region that forms at some finite t_S is described by the outgoing Vaidya metric with decreasing $r_g(v)$. Using it

for the exterior geometry of the shell results in the equation of motion

$$D(R) - \frac{F_V}{F\sqrt{\dot{R}^2 + F}} \left(\frac{1}{2} + \dot{R}\dot{V} \right) = 0, \quad (33)$$

that differs from Eq. (23) in a number of ways.

Close to r_g (and for non-zero \dot{R})

$$\dot{V} \approx -\frac{1}{2\dot{R}} + \frac{F}{\dot{R}^3} \approx -\frac{1}{2\dot{R}} + \frac{X}{\dot{R}^3 r_g}. \quad (34)$$

As a result, the stopping effect of the evaporation is virtually non-existent.

For the shell at rest at $X \ll r_g$, assuming again the Page-like evaporation law

$$\frac{dr_g}{dv} = -\frac{\alpha}{r_g^2}, \quad (35)$$

the radial coordinate acceleration is

$$\ddot{R} \approx -\frac{F'}{2} + \frac{F_V}{F} \approx -\frac{1}{2r_g} + \frac{\alpha}{r_g^2 X}, \quad (36)$$

indicating that evaporation prevents the collapse only if

$$X < \epsilon_* = \frac{2\alpha}{r_g}, \quad (37)$$

that is sub-Planckian even for microscopic black holes.

It is easy to see that for $\dot{R} \neq 0$ the (stopping) acceleration term that is proportional to \dot{V} is much smaller than its classical counterpart. Fig. 2 illustrates this process for the same form of the evaporation $r'_g = -\alpha/r_g^2$ and the same initial data as in the previous case.

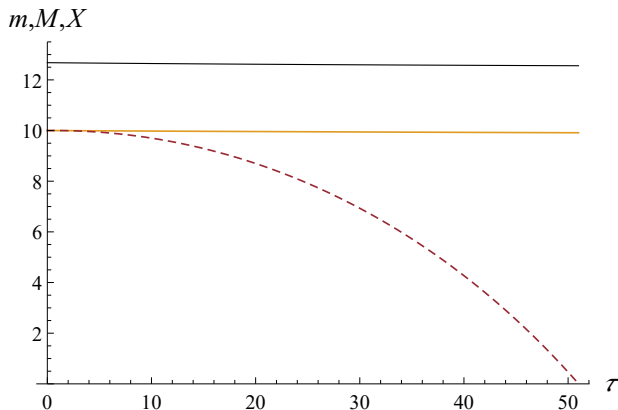


FIG. 2. Horizon crossing. The orange line represents $M(\tau) = r_g(\tau)/2$. The rest mass $m(\tau)$ is shown as the thin black line, and the gap $X(\tau) = R(\tau) - r_g(\tau)$ as the red dashed line. For simulation purposes the evaporation was switched on at $\tau = v = 0$. The initial conditions are $R(0) = 30$ and $\dot{R}(0) = 0$, while $C_0 \equiv C(0) = 20$, and $\alpha = 1$. At the horizon crossing at $\tau_c = 51.010$, the gravitational mass and the rest mass are nearly identical to their initial values: $M(\tau_c)/M(0) = 0.9913$, and $m(\tau_c)/m(0) = 0.9905$, respectively.

Since the influence of evaporation on the dynamics of a macroscopic shell is weak the shell preserves nearly all of its mass at the horizon crossing. We can estimate the proper time of the collapse using the classical equation of motion. However, unlike in the classical scenario, the crossing time according to Bob is finite, as are the propagation time of the last signal that Alice sends before crossing and its redshift. These results are derived in the Appendix.

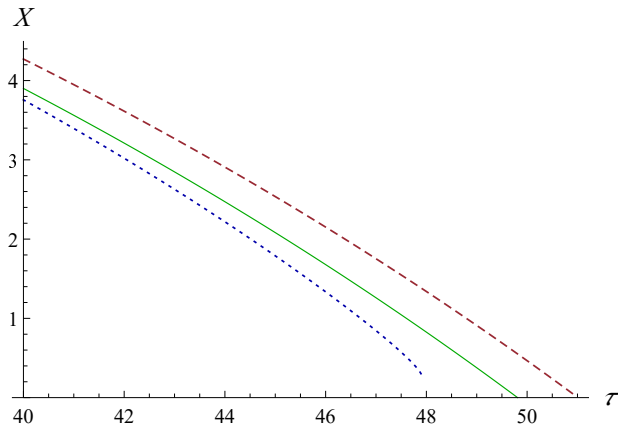


FIG. 3. Comparison of the classical trajectory (thin green line) with exterior geometry given by the outgoing Vaidya metric with $dr_g/du = -\alpha/r_g^2$ (dotted blue line) and the ingoing Vaidya metric with $dr_g/dv = -\alpha/r_g^2$ (dashed red line) at the later stages of the collapse. The initial data is the same as above. In the former case the collapse is accelerated and the shell becomes null at τ_m . In the latter case the collapse is slightly delayed.

The shell approaches r_g in a finite time and with a finite mass. However, the trapped regions that are contained inside the Schwarzschild sphere can only form in finite time of a distant observer if the NEC is violated. A thin dust shell is an approximation of a narrow finite slice of nearly pressureless matter that on the approach to r_g will be increasingly squeezed, resulting in an increased positive energy density. Estimates on the size of the NEC-violating region differ [8, 26, 28], but the shell will not be able to enter it until the final stages of evaporation when the total energy-momentum tensor $T_{\mu\nu} = T_{\mu\nu}^{\text{matter}} + \langle \hat{T}_{\mu\nu}^{\text{radiation}} \rangle$ becomes NEC-violating. However, at this stage the semiclassical theory is likely to break down. Alternatively, the correct dynamics may lead to the contraction or disappearance of the Schwarzschild radius, $f(z, r_g) = 0$, resulting in a compact horizonless object.

IV. DISCUSSION

There is no contradiction between the predictions of different models of thin shell collapse, as they are applicable in different situations. If the spacetime outside the shell is described by an outgoing Vaidya metric with decreasing mass, there is no horizon crossing. This is the expected behaviour of a system that satisfies the NEC. Hence this model describes a radiative process, classical or quantum, but not the final stage of the collapse to a black hole.

Emission of the entire rest mass may indicate either the inapplicability of the thin shell approximation in general, or the appropriateness of a more involved specific model for the shell and/or radiation. A direct consequence of this result is that the geometry outside of a pressureless null shell can never be described by an outgoing Vaidya metric with decreasing mass.

If the geometry outside of the shell is described by an outgoing Vaidya metric with decreasing mass, then the shell approaches the Schwarzschild radius in finite time (both according to the co-moving Alice and distant Bob), losing only an insignificant fraction of its mass. However, so long as the semiclassical approach is valid, the shell cannot cross its Schwarzschild radius and form a trapped region.

It is interesting to note that the quantity $\epsilon_*/2 = |dr_g/dz|_{r_g}$ provides the scale whose multiples characterize different regimes in the thin shell collapse. Its multiples set the scales for horizon avoidance and transition to a null trajectory in the case of the outgoing Vaidya metric, and for the possibility to support a static shell in the ingoing Vaidya geometry.

The above results allow one to argue that the thin shell mod-

els of collapse and evaporation do not have an independent meaning, but simply illustrate their underlying assumptions: If the model corresponds to the impossibility of horizon formation at a finite time, then it will predict horizon avoidance. By the same token, if the model uses the metric that is associated with the finite time appearance of trapped regions, it will predict horizon crossing.

At the approach to r_g the shell still carries positive energy that is incompatible with the finite time formation of horizons and invalidates the model. We will investigate the question of whether or not this is a generic property of a semiclassical theory in future work.

ACKNOWLEDGMENTS

We thank Robert Mann for numerous useful discussions and Joanne Dawson for helpful comments. SM is supported by the iMQRES scheme of Macquarie University.

-
- [1] V. P. Frolov and I. D. Novikov, *Black Holes: Basic Concepts and New Developments*, (Kluwer, Dordrecht, 1998).
 - [2] S. W. Hawking and G. F. R. Ellis, *The Large Scale Structure of the Space-Time*, (Cambridge University Press, 1973).
 - [3] E. Poisson, *A Relativist's Toolkit*, (Cambridge University Press, Cambridge, 2004).
 - [4] M. Visser, Phys. Rev. D **90**, 127502 (2014).
 - [5] B. Krishnam, *Quasi-local horizons*, in A. Ashtekar and V. Petkov, (eds.), *Springer Handbook of Spacetime*, (Springer, NY, 2014), p. 527.
 - [6] F. S. N. Lobo (ed), *Wormholes, Warp Drives and Energy Conditions*, (Springer, 2017).
 - [7] D. Christodoulou, *The Formation of Black Holes in General Relativity*, (European mathematical Society, Zurich, 2009); X. An, arXiv:1703.00118 (2017).
 - [8] R. Brout, S. Massar, R. Parentani, P. Spindel, Phys. Rep. **260**, 329 (1995).
 - [9] A. Ashtekar and M. Bojowald, Class. Quant. Grav **22**, 3349 (2005).
 - [10] J. M. Bardeen, arXiv:1406.4098 (2014); P. Binétruy, A. Helou, and F. Lamy, arXiv:1804.03912 (2018).
 - [11] A. B. Nielsen, Galaxies **2**, 62 (2014).
 - [12] M. Visser, PoS BHs,GRandStrings 2008:001 (2008).
 - [13] C. Barceló, S. Liberati, S. Sonego, M. Visser, JHEP **02**, 003 (2011).
 - [14] A. Paranjape and T. Padmanbhan, Phys. Rev. D **80**, 044011 (2009).
 - [15] C. Barceló, S. Liberati, S. Sonego, M. Visser, Class. Quant. Grav. **23**, 5341 (2006); C. Barceló, S. Liberati, S. Sonego, M. Visser, Phys. Rev. D **77**, 044032 (2008).
 - [16] T. Vachaspati, D. Stojkovic, and L. M. Kraus, Phys. Rev. D **76**, 024005 (2007); T. Vachaspati and D. Stojkovic, Phys. Lett. B **663**, 107 (2008).
 - [17] B. Arderucio-Costa, W. G. Unruh Phys. Rev. D **97**, 024005 (2018).
 - [18] M. Visser and D.L. Wiltshire, Classical Quantum Gravity **21**, 1135 (2004).
 - [19] S. A. Hayward, Phys. Rev. Lett. **96**, 031103 (2006).
 - [20] K. Nakao, C.-M. Yoo, and T. Harada, arXiv:1809.00124 (2018).
 - [21] H. Kawai, Y. Matsuo, and Y. Yokokura, Int. J. Mod. Phys. A **28**, 1350050 (2013); H. Kawai and Y. Yokokura, Int. J. Mod. Phys. A **30**, 1550091 (2015).
 - [22] P.-M. Ho, Nucl. Phys. B **909**, 394 (2016).
 - [23] V. Baccetti, R. B. Mann, and D. R. Terno, Class. Quant. Grav. **35**, 185005 (2018).
 - [24] P. Chen, W. G. Unruh, C-H. Wu, and D.-h. Yeom, Phys. Rev. D **97**, 064045 (2018).
 - [25] R. B. Mann, I. Nagle, and D. R. Terno, Nucl. Phys. B **936**, 19 (2018).
 - [26] V. Baccetti, R. B. Mann, S. Murk, and D. R. Terno, arXiv:1811.04835 (2018).
 - [27] M. Blau, *Lecture Notes on General Relativity*, <http://www.blau.itp.unibe.ch/Lecturenotes.html>.
 - [28] A. Levi and A. Ori, Phys. Rev. Lett. **117**, 231101 (2016).
 - [29] M. K. Parikh and F. Wilczek, Phys. Lett. B **449**, 24 (1999).
 - [30] S. Hossenfelder, L. Modesto, and I. Prémont-Schwarz, Phys. Rev. D **81**, 044036 (2010).

Appendix A: Redshift calculation

Here we disregard the impossibility of crossing the horizon while maintaining a positive energy density and illustrate the collapse model of Sec. III C. We use a linear evaporation law

$$r_g = r_0 - v/\kappa, \quad (\text{A1})$$

that allows for explicit analytical results. Since the shell collapse takes much less time than the evaporation, this is an excellent approximation. To match the Page evaporation law, we set $\kappa = r_g^2/\alpha$.

The equation of an outgoing radial null geodesic

$$\frac{dv}{dr} = \frac{2}{1 - r_g(v)/r} \quad (\text{A2})$$

separates after the change of variables ($v = r\tilde{v} + C_0\kappa$) and its general solution can be written as

$$K = -2\sqrt{\frac{\kappa}{8+\kappa}} \operatorname{arctanh} \left[\sqrt{\frac{\kappa}{8+\kappa}} \left(1 + \frac{4r}{\kappa(r-r_0)+v} \right) \right] + 2 \ln r + \ln \left(1 + \frac{\kappa^2 r_0(r-r_0) + \kappa(2r_0-r)v - v^2}{2\kappa r^2} \right), \quad (\text{A3})$$

where K is the integration constant.

We first use this result to evaluate the redshift that is suffered by the signal sent by Alice at the horizon crossing. Since the evaporation law is linear we can adjust parameters such that the crossing happens at $V = 0$ at $r_g(0) = r_0$. For the light emitted by Alice at $\Delta\tau$ before the crossing, the constant is given by in the leading order as

$$K = \pi i - \frac{4\pi i}{\kappa} + 2 \ln r_0 + \frac{\Delta\tau}{r_0} \left(\frac{1}{2|\dot{R}_0|} + 2|\dot{R}_0| \right), \quad (\text{A4})$$

where we also expanded in powers of κ , using that $\kappa \gg 1$, and $\dot{R}_0 = \dot{R}(0)$.

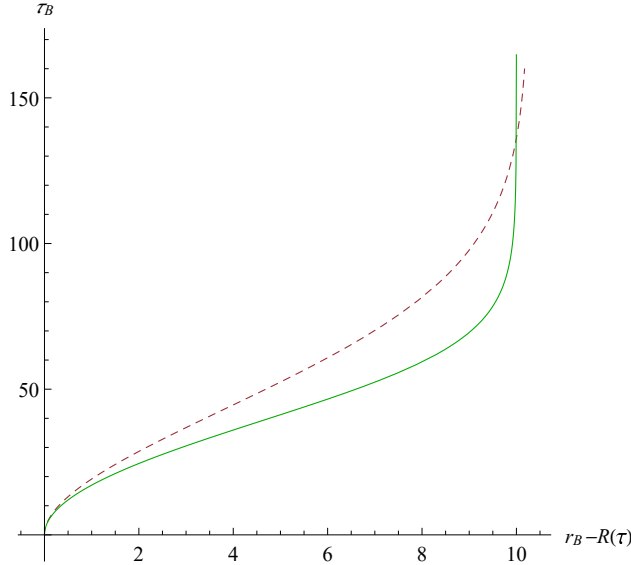


FIG. 4. Time of arrival of Alice's signals to Bob. The green line represents the classical case $r_g = r_0 = \text{const.}$ The dashed red line represents the case with the linear evaporation law with $\kappa = 1/400$. In this case the last ray reaches Bob at $\tau_B = 160$.

To show that the transmission time and the redshift are finite, we consider a particular position of Bob that makes the calculations particularly simple. To this end we locate Bob at the position r_B that the light emitted at $v = 0$ reaches at $v_B = \kappa r_0$, i.e. when the shell completely evaporates. Consider the beam that arrived at the same location Δv earlier. Then we have (again using $\kappa \gg 1$)

$$K = \pi i - \frac{4\pi i}{\kappa} + 2 \ln r_B - 2 \ln \kappa + \frac{8 \ln \kappa - 8 - \ln 256}{\kappa} + \frac{\Delta v}{r_B}. \quad (\text{A5})$$

Comparison of the zeroth order terms identifies Bob's location,

$$r_B \approx \frac{1}{2}\kappa r_0 - (2 \ln \kappa - 2 - \ln 4)r_0 + \dots, \quad (\text{A6})$$

while the leading order term in the redshift is determined by

$$\frac{dv}{d\tau} = \frac{(1 + 4\dot{R}_0^2)r_B}{2|\dot{R}_0|r_0}. \quad (\text{A7})$$

We recall that $|\dot{R}| \leq 3/4$, and since

$$d\tau_B = \sqrt{f(v, r_B)}dv_B \approx dv_B, \quad (\text{A8})$$

we see that the redshift is of the order of κ . If we assume that the initial radius of the shell R_A satisfies $r_0 \ll R_A < r_B$, we have $|\dot{R}_0| = 3/4$ and

$$\frac{dv}{d\tau} = \frac{13}{12}\kappa. \quad (\text{A9})$$

The time of arrival of the signals that are sent by Alice as the function of her progress is represented in Fig. 4. Here the Bob is located at the initial position of Alice, $r_B = R_A$. His proper time is calculated according to

$$\tau_B = \int_0^v \sqrt{f(v', r_B)}dv'. \quad (\text{A10})$$

We see that the last signal that is sent by Alice before she crosses the Schwarzschild sphere reaches Bob in a finite time, while in the classical case this time diverges as Alice approaches r_g .